

# **A safer disposal of hazardous phosphate coating sludge by formation of an amorphous calcium phosphate matrix**

I. Navarro-Blasco<sup>a</sup>, A. Duran<sup>a</sup>, M. Pérez-Nicolás<sup>a</sup>, J.M. Fernández<sup>a</sup>, R. Sirera<sup>a</sup>, J.I. Alvarez<sup>a\*</sup>

*<sup>a</sup>MIMED Research Group; Department of Chemistry and Soil Sciences, School of Sciences, University of Navarra.*

*Irunlarrea, 1. 31008 Pamplona, Spain*

## **Abstract**

Phosphate coating hazardous wastes originated from the automotive industry were efficiently encapsulated by an acid-base reaction between phosphates present in the sludge and calcium aluminate cement, yielding very inert and stable monolithic blocks of amorphous calcium phosphate (ACP). Two different compositions of industrial sludge were characterized and loaded in ratios ranging from 10 to 50 wt.%. Setting times and compressive strengths were recorded to establish the feasibility of this method to achieve a good handling and a safe landfilling of these samples. Short solidification periods were found and leaching tests showed an excellent retention for toxic metals (Zn, Ni, Cu, Cr and Mn) and for organic matter. Retentions over 99.9% for Zn and Mn were observed even for loadings as high as 50 wt.% of the wastes. The formation of ACP phase of low porosity and high stability accounted for the effective immobilization of the hazardous components of the wastes.

**Keywords:** calcium aluminate cement; heavy metals; waste management; zinc; leaching; solidification/stabilization

\*Corresponding author:

Dr. José Ignacio Alvarez

Dpto. de Química y Edafología

Facultad de Ciencias, Universidad de Navarra

C/ Irunlarrea, 1, 31.008 Pamplona (Navarra), Spain

Phone: 34 948 425600; Fax: 34 948 425670

e-mail: [jalvarez@unav.es](mailto:jalvarez@unav.es); [mimed@unav.es](mailto:mimed@unav.es)

## **1. Introduction**

The automotive industry originates wastes such as shredder residue (Péra et al., 2004), paint (Arce et al., 2010) or phosphate coating sludge (PS) (Dogan and Karpuzcu, 2010; Ucaroglu and Talinli, 2012). Phosphating is the most widely applied system for metal pretreatment process. Surface modification is one the methods to prevent metal from corrosion. During a phosphating process, a metal surface is treated with the aim of giving rise to a hard and electrically non-conducting surface coating of insoluble phosphate (Sankara, 2005). PS is a residue from the surface treatment of metals, basically containing water, ferrous and zinc phosphates and other minor elements such as Ni, Na, K, S, Pb, Cr and Cu (Caponero and Tenório, 2000). Different types of phosphate coatings have been introduced and there are also a lot of special additives (such as zinc carbonate, sodium lignosulphonate, thiourea,...) used in phosphate baths that can yield final wastes with different compositions and potential toxicities (Sankara, 2005). Of course, different operating parameters and in-process modifications could also render final wastes with diverse compositions and degree of health hazard. Nevertheless, within the field of automotive industry, PS has been often reported to be one of the most problematic varieties of waste, due to the possible leaching of the heavy and/or transition metals which contains (Dogan and Karpuzcu, 2010; Ucaroglu and Talinli, 2012). Accordingly, it has been classified as a hazardous waste by the U.S. Environmental Protection Agency (EPA) and the European Union. In agreement with the current regulations, this waste must be encapsulated or treated before disposing it in a landfill.

Different methodologies for stabilization/solidification (S/S) of inorganic hazardous wastes and following landfill have been fruitfully applied. Regarding the S/S treatment of PS, scarce studies have been reported in the literature. In all of them, authors have used ordinary Portland cement (OPC) as binder (Dogan and Karpuzcu, 2010; Ucaroglu and Talinli, 2012; Pinarli et al., 2005). Different formulation of paint wastes -from the automobile industrial sector- with lime, lime-coal

fly-ash and lime-Portland cement were carbonated and studied to assess the effectiveness of the S/S processes (Arce et al., 2010).

It must be considered that organic matter and other compounds present in polluted sludge and other dangerous wastes can interfere with the hydration and setting process of the Portland cement. Phosphates, for instance, have been reported to act as inhibitors of the setting process (Pinarli et al., 2005). As detrimental consequences of this interference can be mentioned the inability of the system to set and to effectively encapsulate the hazardous materials, the increase in porosity and a parallel reduction in compressive strength that, at short and medium term, leads to an increased release of the toxic compounds and a clear decrease of the integrity and stability of the binding matrix. Therefore, alternative binders to OPC are receiving growing attention to encapsulate hazardous materials. A mix of mayenite ( $C_{12}A_7$ ) and OPC has been tested as a matrix to encapsulate sludge from a sewage treatment plant (Zhen et al., 2012). The high efficiency of calcium aluminate cement (CAC) as retainer of toxic metals has been assessed (Navarro-Blasco et al., 2013a; Navarro-Blasco et al., 2013b). CAC offers particularly interesting properties such as high early strength, resistance to chemical attack and to abrasion, refractory properties, and low ambient temperature placement (Ukrainczyk et al., 2012). The mineralogical and chemical composition of CAC substantially differs from OPC. Hardening of CAC is primarily due to hydration of anhydrous phases such as CA,  $CA_2$  and  $C_{12}A_7$ , yielding the metastable hexagonal phases  $CAH_{10}$ ,  $C_2AH_8$  and amorphous aluminium hydroxide, which is followed by the formation of the stable cubic phases  $C_3AH_6$  and  $AH_3$ , in a highly temperature dependant process (Ukrainczyk et al., 2012). A variant of CAC binder is that derived from acid-base reaction between acidic phosphate solutions and base reactant CAC, forming polyphosphate-CAC matrices, which show some advantages in comparison with unmodified CAC specimens (Sugama and Carciello, 1991; Sugama and Carciello, 1995; Swift et al., 2013a; Swift et al., 2013b; Fernández et al., 2014).

Usually, the assessment of the ability of a S/S process involves different issues: (i) the physical properties of the S/S products, the consistency and setting time of the fresh-state matrix and compressive strength tests of the hardened samples, to gain understanding about the handling, stability and integrity of the specimen including the encapsulated waste; (ii) the elucidation of the chemical interactions between the hydrated compounds of the binding system and the components of the waste. In this case, a complete microstructural characterization is necessary to gain deeper knowledge about the mechanisms implied in the interactions among the different agents in the systems cement binders-sludge; and (iii) the solid, leachable and soluble chemical characterization of the S/S products by knowing the leachability indices and the diffusion coefficients (Silva et al., 2011).

This work is dealt with the effective encapsulation of two different automotive phosphate coating sludge in CAC-based mortars. Our aim was to provide a new final fate for these PS as an alternative to the currently used one, which is accumulation into a dam that poses serious environmental risks. The rationale is that polyphosphate-CAC matrices have shown interesting potential to solidify/stabilize heavy metals, owing to the aforementioned acid-base reaction that yields a compact and low porous matrix mainly composed of ACP - amorphous calcium phosphate -, which can be able to retain hazardous compounds. We aimed to take advantage of the reactivity of one of the sludge components: the sludge with relatively large concentrations of phosphate is expected to act themselves as reactants that, interacting with the CAC, could result in a very effective retaining system of the sludge constituents. Sludge samples from two locations have been incorporated in high proportion within the mix. We discussed the effects of the sludge on the CAC mortar and a possible interaction mechanism is provided.

## **2. Materials and methods**

### **2.1. Raw materials and mortar preparation**

A total of 10 different batches of specimens were prepared by mixing a calcium aluminate cement (Electroland<sup>®</sup>, Ciments Molins, Spain) with two different PS (a paler one, white sludge, WS, and a darker one, brown sludge, BS) coming from the automotive industry. A sand of siliceous nature was used as aggregate. Chemical and mineralogical composition of the CAC as well as of the sand was reported elsewhere (Fernández et al., 2014). Different sludge waste/CAC weight ratios were used, as collected in Table 1. A control group with sodium hexametaphosphate (SHMP,  $(\text{NaPO}_3)_6$ ), as a pure acidic phosphate reactant, was also prepared for comparison purposes.

Raw materials were blended for 5 min in a mixer. The CAC/sand ratio was 1/1.5 by weight. The required mixing water to achieve the consistency of the control sample was also detailed in Table 1. Fresh mixtures were decanted into cylindrical PVC molds (5 x 3.5 cm) and subjected to a curing regime of 20 °C and 95% RH for 7 and 28 days. To guarantee the statistical significance, three specimens of each one of the samples for each curing age were prepared.

## **2.2. Experimental procedures**

The sludge wastes were fully characterized by chemical analysis. Samples were placed into a high-pressure Teflon bomb, digested by a 3:1 mix of  $\text{HNO}_3$  (69 wt.%) and  $\text{HCl}$  (32 wt.%) and treated in a closed microwave system. The acidic solution allowed us to determine major and minor components of the sludge by means of atomic absorption spectrometry (AAS, Perkin-Elmer AAnalyst-800).

Conductivity and pH values (Thermo-Orion) were measured in an aqueous suspension of the sludge (1:5 weight ratio). Several analytical methodologies were used to characterize the raw sludge, according to procedures described elsewhere (Fernández et al., 2014): FTIR-ATR; thermal studies; X-ray diffraction studies; and SEM-EDAX examinations. Organic matter contents were calculated by the weight loss in the TG curve that showed a minimum in the DTG

curve at ca. 550°C and further confirmed by calcination according to a norm (TMECC Method, 2001).

Consistency of the freshly prepared mortars was assessed by slump obtained through the flow table test (EN-1015-3, 2000). Setting time was recorded according to the norm (EN-1015-9, 2000). In hardened mortars, unconfined compressive strengths (rate loading of 50 Ns<sup>-1</sup>), and both total porosities and pore size distributions (by mercury intrusion porosimetry, MIP, Micromeritics AutoPore-9500) were measured (Fernández et al., 2014). In addition, XRD and SEM-EDAX studies were also carried out as above mentioned.

The leachability of the raw sludge wastes by water was studied by using EN 12457-4 extraction test method (EN-12457-4, 2002). The leaching performance of the monolithic specimens was determined by means of the semi-dynamic Tank Test (EA NEN 7375, 2004), as fully described elsewhere (Lasheras-Zubiate et al., 2012). The concentration levels of the elements and organic matter were measured, respectively, by AAS and by the analysis of total organic carbon content in filtrates was analyzed using a LiquiTOCII Analyzer (Elementar).

### **3. Results and discussion**

#### **3.1. Characterization of the phosphate coating sludge**

Table 2 collects the chemical analysis of the two tested sludges. The pH values of the aqueous suspensions (1:5 sludge/water ratio) as well as the conductivity of the supernatants can be seen in Table 3. The results showed that organic matter contents were significant in the two WS and BS sludge, above 20%, with 29.7% as average value for BS and a lower percentage (21.6%) for WS sample.

Regarding the phosphate determination, both polluted sludge yielded relevant amounts of phosphate, which were expected to be present as hydrogenphosphate salts, owing to the similar and slightly acidic pH of the samples (value of 5.5).

However, the WS revealed almost 50% of its composition as phosphate whereas the BS reached only a 20% of phosphate. Another outstanding difference was found in sample BS, which showed around 10 wt.% of carbonates in its composition, whereas for sample WS negligible amount of this anion was determined. The proper identification of carbonates was carried out by means of thermal analysis and FTIR. TG- DTG results allowed us to see for the BS sample an endothermic weight loss at ca. 750°C, which can be ascribed to the carbonate decomposition (Fig. 1). FTIR spectrum of this sample showed absorption bands at ca. 1500-1400  $\text{cm}^{-1}$  (asymmetric stretching,  $\nu_3$ ), 875  $\text{cm}^{-1}$  (out-of-plane bending,  $\nu_2$ ) and 712  $\text{cm}^{-1}$  (planar bending,  $\nu_4$ ) that can be attributed to different normal modes of carbonate (Fig. S1 in the Supplementary material) (Adler and Kerr, 1963). On the contrary, sample WS did not show evidences of carbonates in its composition, with no decomposition phenomena between 600-900°C (Fig. 1) and no absorptions bands at the mentioned wavelengths in the FTIR spectrum.

Taking into account the large percentage of calcium in BS sample as compared with WS sample and the decomposition temperature the presence of calcium carbonate as the main carbonated phase can be inferred. This fact was further confirmed by XRD analysis of this BS sample, indicating the presence of calcite ( $\text{CaCO}_3$ ) by its main diffraction peak (Fig. S2 in the Supplementary material).

In connection with the toxic metals amounts, Cu, Mn, Ni, Cr and specially Zn were the most abundant hazardous metals found in the samples. These results are in good agreement with the results reported in previous works for similar wastes (Dogan and Karpuzcu, 2010; Ucaroglu and Talinli, 2012; Caponero and Tenório, 2000; Pinarli et al., 2005), as PS are mainly composed of zinc phosphates coming from decanter baths of phosphate, very commonly used in the industry responsible for this kind of wastes. Both sludges can be classified as hazardous wastes, due to their reactive and toxic characteristics according to the regulations and cannot be landfilled without a previous S/S process (Ucaroglu and Talinli, 2012). The WS showed the largest concentrations of the toxic metals. The chemical composition of WS indicates a larger amount of metallic phosphates as compared with the BS, which is in line with the higher conductivity of the supernatant fraction.

All these facts point to WS as the most hazardous waste, owing to its high toxic metals concentrations and their mobility that increases its leaching potential. Textural examinations the sludge were carried out by SEM observations (Fig. 2a and 2b), showing the larger degree of compactness of the BS. EDAX analyses confirmed the chemical composition (Fig. 2c and 2d).

### **3.2. Effect of the sludge encapsulation on the properties of the mortars**

Regarding the properties of the mortars in the fresh state, Table 4 shows that control mortar (prepared by mixing CAC and sodium hexametaphosphate in 20 wt.% with respect to cement weight) offered 138 mm as the slump value obtained after performing the flow table test. This value with a 10% of deviation was taken as the targeted consistency. The incorporation of the sludge increased the water demand in order to achieve this slump: the larger the percentage of sludge, the higher the required mixing water (Table 1). This fact was a physical consequence of the small particle size of the sludge compounds, which, after being mixed with the binding matrix, reduced the workability of the sample adsorbing the mixing water onto the surface of the particles, thus hindering the lubricant role of the free water.

A significant parameter related to the handling of the cement-based S/S systems is the setting time: the interference of toxic metals, sludge, sewage waters ... with the cement hydration, delaying or even preventing the setting of the fresh mixture, can lead to an insurmountable obstacle, since solidification cannot be reached in a reasonable period of time. The control mortar showed a very short setting time (6 min), which echoed the values reported for the phosphate-bonded calcium aluminate cements (Sugama and Carciello, 1991; Sugama and Carciello, 1995; Swift et al., 2013b). The presence of either WS or BS induced a delay in the setting time (Table 4). This delay can be ascribed to the toxic metals presence in the sludge (Cu and Zn, specially), which acted as inhibitory compounds of the setting process (Navarro-Blasco et al., 2013a). The organic matter could also interfere somewhat with the hydration, as confirmed by the longer delays observed for BS samples, with larger amounts of organic compounds, as compared with WS samples. However, it



must be noticed that the hardening of the mortars always took place below 100 min and in the majority of the samples below 60 min, so that the handling of these matrices was not difficult. For comparison purposes, literature has reported, when Portland cement was used as solidifying matrix, setting times well above 400 min for samples with just 10 wt.% of sludge (Pinarli et al., 2005) or extremely long solidification periods higher than 28 days (Ucaroglu and Talinli, 2012).

Compressive strength of the samples was measured after 7 and 28 curing days and the collected values can be observed in Fig. 3. The compressive strength underwent a reduction when either WS or BS was added to the mortar as compared with the control sample. In the reference sample, pure sodium hexametaphosphate (acidic compound) added quickly reacted with the CAC (basic compound) yielding a strong and low porosity matrix (Swift et al., 2013a; Fernández et al., 2014). Given that wastes are composed of lower percentages of phosphates and present heavy metals and organic matter, the strength reduction was an expected result, in good agreement with previous works on S/S processes of phosphate sludge into cement matrices (Dogan and Karpuzcu, 2010; Ucaroglu and Talinli, 2012; Pinarli et al., 2005). Comparatively, the BS induced a stronger reduction, which is in line with the more intense interference with the setting process observed for these samples. The white sludge showed better strength performance and this fact can be related to the higher phosphate amounts of this sludge and its lower organic matter contents in comparison with the brown sludge. In spite of the foreseeable strength reduction, it must be noticed that the tested mortars showed compressive strength values above the minimum value of 1 MPa, which is the threshold value for landfilling solid wastes (Environment Agency, 2010). Furthermore, the regulation for secondary waste forms requires a compressive strength of at least 3.45 MPa, which was also fulfilled by all the mortars (U.S. Nuclear Regulatory Commission, 1991). The fate of these materials including the sludge could also be the obtaining of controlled low-strength materials, used as backfills, with unconfined compressive strength  $\leq 8.3$  MPa ( $\leq 1.4$  MPa if the application requires removal at a later date) (IR 18-1, 2011) under condition of no adverse environmental effects as will be assessed below.

The XRD studies (Fig. 4) showed that in the control mortar (with pure SHMP) only diffraction peaks of quartz (from the sand) ( $26.67$  and  $20.86^\circ 2\theta$ ), anhydrous CA ( $30.08$  and  $30.15^\circ 2\theta$ ), aluminum phosphate ( $27.65^\circ 2\theta$ ) and  $\text{CAH}_{10}$  ( $25.00^\circ 2\theta$ ) were identified. The presence of polyphosphates gave rise, in accordance with previous works (Swift et al., 2013b; Fernández et al., 2014), to the formation of an amorphous calcium phosphate (ACP) phase as evidenced by two findings: (i) the development of an amorphous XRD pattern, and (ii) the absence of significant diffraction peaks of hydrated calcium aluminates given that phosphates had been reported to interfere the hydration of calcium aluminate-based phases (in the control sample just one peak of  $\text{CAH}_{10}$  could be seen). The ACP phase was responsible for the fast setting and the large strength of this mortar yielding a low porosity matrix, as can be seen in its pore size distribution (Fig. 5) and in its total porosity value (8.7%, Table 5). This unimodal distribution showed at ca.  $0.05 \mu\text{m}$  the mean pore diameter, without other significant meso- or macropores.

The incorporation of the WS also resulted in the amorphization of the binding phase and the absence of diffraction peaks of hydrated calcium aluminates (Fig. 4). The presence of phosphates inhibited the hydration of CAC, forming ACP instead. Only slight amounts of anhydrous CA could be identified (main diffraction peaks at  $30.08$  and  $30.15^\circ 2\theta$ ). In addition, a phosphate-based compound (aluminum phosphate, ICDD 01-076-0233 with main diffraction peak at  $27.65^\circ 2\theta$ ) also appeared as a further confirmation of the acid-base reaction between phosphates of the sludge and the basic CAC. This phase had also been found in SHMP-CAC systems (Fernández et al., 2014). MIP measurements showed that the higher the amount of WS, the higher the porosity in the pore range of  $0.15\text{-}4 \mu\text{m}$ . At the same time, the macroporosity in the range of  $5\text{-}50 \mu\text{m}$  also increased (Fig. 5a). These two increments gave rise to an increase in the overall porosity of the monolithic specimens, responsible for the strength drop, as can be seen in Table 5. Large WS additions (30, 40 and 50 wt. %) caused an excessively porous matrix owing to the large

amount of sludge that could not fully react with the CAC. These samples showed total porosity values beyond 25% (Table 5).

Similarly, the incorporation of increasing amounts of BS offered amorphous XRD patterns (Fig. 4). Depending on the sludge load, calcium carbonate as calcite can be seen (diffraction peak at  $29.42^\circ 2\theta$ ). The aluminum phosphate diffraction signal was also identified. Large porosity values were observed for these mortars (Table 5) and PSDs showed an increase in the pores between 1 and 10  $\mu\text{m}$ . The increase in the population of pores at ca. 0.01  $\mu\text{m}$  that can be seen especially for large BS percentages could be ascribed to the pores of the solid compounds of the sludge (Fig. 5b). Large BS amounts showed a limited reaction with CAC.

SEM examinations showed the presence of a relatively homogeneous structure when WS was added at low percentages (10 wt. %) (Fig. 6a). At high WS percentages (50 wt.%), the porosity of the matrix and the heterogeneity clearly increased, in agreement with the PSD and compressive strength results (Fig. 6b). Details of the matrix allowed us to observe a binding matrix interconnected by a fibrous network (Fig. 6c) or, in other areas, the interconnected binding matrix was seen as a flaky, honeycomb-shaped microstructure of low porosity (Fig. 6d). The appearance of this matrix can be reasonably ascribed to the ACP phase formation, explaining the XRD results (Julien et al., 2007). This fact was confirmed by: (i) EDAX analysis of the individual areas of these two morphological structures that showed the simultaneous presence of large amounts of P and Ca (Fig. 6e and 6f); and, (ii) the elemental mapping by EDAX, which evidenced a distribution in which P was associated to Ca (and also Al) (Fig. 7). Toxic metals of the WS, Zn especially but also Mn and Ni, also appeared bonded to this phase (Figs. 6e, 6f and 7).

The incorporation of BS gave rise to a matrix with larger pores, in line with the PSD measurements (Fig. 8a and 8b). Examination at higher magnification showed  $\text{CAH}_{10}$  hexagonal plate-like crystals embedded in the matrix (Navarro-Blasco et al., 2013b) (Fig. 8c) and also the

fibrous network as well as the honeycomb-shaped areas related to ACP (Fig. 8d and 8e, respectively) although to a lesser extent than in WS samples.

EDAX analyses also indicated the association between P and Ca (Fig. 9), confirming the reaction between the phosphate groups of the sludge and the CAC. Zn also was found attached to this phase (Fig. 9). Sometimes, spots of unreacted Zn phosphates also appeared as a consequence of a lower degree of phosphate-CAC reaction (Fig. 10). However, Ni appeared preferentially attached to the ACP phase.

### **3.3. Leaching**

Measurements of the extractions by water of the raw sludge following the extraction test method (EN 12457-4, 2002) (Table 6) showed that, in general, significant amounts of toxic metals (Zn, Ni, Cr, Cu...) and organic matter were released, as proper to a hazardous wastes. Tolerable levels of Zn and Ni according to the European Council decision (2003/33/EC, 1991) were largely surpassed for WS, as evidenced in Table 6. The release of toxic metals was even larger when extraction with acidic media (HCl 0.1M) was carried out, simulating a potential scenario of acidic run-off of the sludge. The organic matter release was extremely high for BS, beyond the acceptance limits for landfilling of hazardous wastes (2003/33/EC, 1991), in good agreement with the large organic matter amounts determined for this sludge.

By contrast, leaching results obtained from the tank test of the sludge after reaction with the CAC showed a quasi-complete retention of those very same metals (Table 7) and a strong reduction of the organic matter concentrations in the leachates (Table 8) in comparison with the data from the extraction test reported in Table 6. This behaviour was followed by both WS and BS. Zn and Mn showed a particularly high affinity for the ACP matrix and retention percentages were higher than 99.9% even for sludge dosages as high as 50%. This performance is strikingly diverse from that reported for solidification in ordinary Portland cement (Ucaroglu and Talinli,

2012), in which a PS load of just 10 wt. % resulted in 98.74% retention of Zn as the most favourable figure and 39.47% of Cr and 35% of Cu as the lowest retention values. Similarly, Pinarli et al. (2005) reported 2.9% and 1.8% of leaching for Zn and Ni, respectively, for only a 5 wt.% of sludge load, what means a retention of 97.1% and 98.2% for those metals. On the contrary, in this work, reaction between phosphate contained in the sludge and CAC provided an optimum binding matrix to solidify/stabilize the toxic metals as well as the organic matter of the PS in a very effective way, even for much higher loadings.

In order to explain the interaction of the toxic metals with the stabilizing matrix, two pathways can be invoked: i) interaction with the ACP phase, as depicted in EDAX analyses in Figures 6e, 6f, 7 and 9 for Zn and in Fig. 10 for Ni, in which both metals appeared associated to the ACP; ii) the insolubility of the phosphates of several of the toxic metals, specially for high dosages of sludge. In these cases, spots of insoluble metallic phosphates were physically encapsulated within the ACP (Fig. 10 for Zn), in a low-porosity matrix.

In connection with these retention routes, the study of the leaching mechanisms, according to the Tank Test norm (EA NEN 7375, 2004), showed that P, Ca and Zn were globally released through a similar dissolution mechanism, as can be seen in the slope values reported in Table 9. This overall dissolution mechanism is coherent with the blockage of Zn within the ACP matrix: only the small soluble fraction of the ACP matrix gave rise to small amounts of Zn and P measured in the leachates. In this sense, the stability of the binding matrix in hardened specimens could also be seen by the improved retention of phosphate anions when compared with the control group prepared with SHMP. This retention was close to 100% irrespectively of the sludge dose (Table 7). These data should be interpreted keeping in mind the large phosphate contents of the assayed sludge, either WS or BS, proving the capacity of CAC to chemically interact by acid-base reaction with these phosphates groups and thus completely retaining them in the cementitious blocks. The experimental findings support the high stability and low

solubility of the ACP matrix that guarantees an efficient retention of Zn, as the most representative toxic metal in the sludge. Taking into account these release performances as well as the fresh- and hardened-state properties of the samples, we can suggest the incorporation of PS up to 30 wt.% in CAC as the optimum degree of load. In addition, it is clear from the presented data that the monolithic specimens obtained as a result of the S/S method proposed in this paper can be safely managed and landfilled according to the norms.

#### **4. Conclusions**

This work describes an application of calcium aluminate cement. A quick and safe inertization of two industrial PS wastes was developed and tested. The reaction between the phosphates of the wastes and calcium aluminate cement was used as the main solidifying process, as it was proved to yield a stable and low-porosity matrix mainly composed of ACP. This reaction took place in short periods of time, reaching solidification in 44 min on average. Unconfined compressive strengths of the monolithic specimens showed that they can be safely disposed of to landfill because they fulfilled the threshold value of the regulations. Other uses as secondary waste forms or controlled low-strength materials could also be the fate of these materials according to their mechanical performance.

Leaching tests indicated that, for the two sludge wastes and irrespective of the sludge dosage, toxic metals such as Zn, Ni, Cr, Cu and Mn were almost fully retained within the binding matrix together with the largest fraction of the organic matter. For example, Zn and Mn yielded retention percentages greater than 99.9%. Regarding Zn as the most representative toxic metal, SEM-EDAX analyses proved its interaction with the ACP phase. Studies of the leaching mechanisms of P, Ca and Zn showed that dissolution was the main governing process. Therefore, the very low concentrations found in the leachates were ascribable to the almost negligible

dissolution of the matrix, which has been proved to be very stable and efficient to successfully solidify/stabilize these hazardous wastes.

### **Acknowledgements**

This work was fully funded by Fundación Universitaria de Navarra (grant FUNA2013-15108402). We are also grateful to LURESA for providing complementary funding (grant LUR-2010) and to Dr. M.C. Jimenez de Haro (ICMS) for helping in SEM analyses. Leaching experiments were carried out by P. Margallo as part of her final degree project.

### **References**

- Adler, H.H., Kerr, P.F. Infrared absorption frequency trends for anhydrous normal carbonates, *Am. Mineral.* 48 (1963), pp. 124-137.
- Arce, R., Galán, B., Coz, A., Andrés, A., Viguri, J.R. Stabilization/solidification of an alkyd paint waste by carbonation of waste-lime based formulations, *Journal of Hazardous Materials* 177 (2010), pp. 428-436.
- Caponero, J., Tenório, J.A.S. Laboratory testing of the use of phosphate-coating sludge in cement clinker, *Resources, Conservation and Recycling* 29 (2000), pp. 169-179.
- Dogan, O., Karpuzcu, M. Recovery of phosphate sludge as concrete supplementary material, *Clean-Soil, Air, Water*, 38 (2010), pp. 977-980.
- EA NEN 7375 Leaching Characteristics of Moulded or Monolithic Building and Waste Materials. Determination of Leaching of Inorganic Components with the Diffusion Test, 2004.
- EN 12457-4: Characterization of Waste-Leaching; Compliance test for leaching of granular waste materials and sludges, 2002.
- EN-1015-3, Methods of Test Mortar for Masonry. Part 3: Determination of Consistence of Fresh Mortar (by Flow Table), 2000.
- EN-1015-9, Methods of Test Mortar for Masonry. Part 9: Determination of Workable Life and Correction Time of Fresh Mortar, 2000.
- European Council decision, 2003/33/EC establishing criteria and procedures for the acceptance of waste at landfills pursuant to article 16 of and Annex II to Directive 1999/31/EC, 1991.

Fernández, J.M., Navarro-Blasco, I., Duran, A., Sirera, R., Alvarez, J.I. Treatment of toxic metal aqueous solutions: encapsulation in a phosphate-calcium aluminate matrix, *J. Environ. Manage.* 140 (2014), pp. 1-13.

IR 18-1 Use of Controlled Low Strength Material (CLSM) as controlled fill (California Department of General Services Division of the State Architect Interpretation of Regulations Document, 2011.

Julien, M., Khairoun, I., LeGeros, R.Z., Delplace, S., Pilet, P., Weiss, P., Daculsi, G., Bouler, J.M., Guicheux, J. Physico-chemical–mechanical and in vitro biological properties of calcium phosphate cements with doped amorphous calcium phosphates, *Biomaterials*, 28 (2007), pp. 956-965.

Lasheras-Zubiarte, M. Navarro-Blasco, I., Fernández, J.M., Alvarez, J.I. Encapsulation, solid-phases identification and leaching of toxic metals in cement systems modified by natural biodegradable polymers, *Journal of Hazardous Materials* 233–234 (2012), pp. 7-17.

Navarro-Blasco, I., Duran, A., Sirera, R., Fernández, J.M., Alvarez, J.I. Solidification/stabilization of toxic metals in calcium aluminate cement matrices, *Journal of Hazardous Materials* 260 (2013) (a), pp. 89-103.

Navarro-Blasco, I., Fernández, J.M., Duran, A., Sirera, R., Álvarez, J.I. A novel use of calcium aluminate cements for recycling waste foundry sand (WFS), *Construction and Building Materials* 48 (2013) (b), pp. 218-228.

Péra, J., Ambroise, J., Chabannet, M. Valorization of automotive shredder residue in building materials, *Cement and Concrete Research* 34 (2004), pp. 557-562.

Pinarli, V., Karaca, G., Salihoglu, G., Salihoglu, N.K. Stabilization and solidification of waste phosphate sludge using portland cement and fly ash as cement substitute, *Journal of Environmental Science and Health. Part A, Toxic/Hazardous substances & environmental engineering* 40 (2005), pp. 1763–1774.

Sankara, T.S.N., Surface pretreatment by phosphate conversion coatings – A review, *Rev. Adv. Mater. Sci.* 9 (2005) 130-177.

Silva, M.A.R., Testolin, R.C., Godinho-Castro, A.P., Correa, A.X.R., Radetski, Environmental impact of industrial sludge stabilization/solidification products: Chemical or ecotoxicological hazard evaluation?, *Journal of Hazardous Materials* 192 (2011), pp. 1108-13.

Sugama, T., Carciello, N.R., Sodium phosphate-derived calcium phosphate cements, *Cement and Concrete Research* 25 (1995), pp. 91–101.

Sugama, T., Carciello, N.R., Strength development in phosphate-bonded calcium aluminate cements, *J. Am. Ceram. Soc.* 74 (1991), pp. 1023–1030.

Swift, P., Kinoshita, H., Collier, N.C. The effect of supplementary pulverised fuel ash on calcium aluminate phosphate cement for intermediate-level waste encapsulation, in: F. Bart, C. Cau di Coumes, F. Frizon, S. Lorente (Eds.), *Cement-based Materials for Nuclear Waste Storage*, Springer Science+Business Media, New York (2013) (a), pp. 215–224.



Swift, P., Kinoshita, H., Collier, N.C., Utton, C.A. Phosphate modified calcium aluminate cement for radioactive waste encapsulation, *Adv. Appl. Ceram.* 112 (2013) (b), pp. 1–8.

TMECC Method 05.07.2001. Organic matter. In: The United States Composting Council. *Test Methods for the Examination of Composting and Compost*, New York, USA, 2001.

U.S. Nuclear Regulatory Commission Waste Form Technical Position, 1991.

Ucaroglu, S., Talinli, I. Recovery and safer disposal of phosphate coating sludge by solidification/stabilization, *Journal of Environmental Management* 105 (2012), pp. 131-137.

Ukrainczyk, N., Vrbos, N., Sipusic, J. Influence of metal chloride salts on calcium aluminate cement hydration, *Advances in Cement Research* 24 (2012), pp. 249-262.

Waste acceptance at landfills, Environment Agency, Bristol, 2010.

Zhen, G., Lu, X., Cheng, X., Chen, H., Yan, X., Zhao, Y. Hydration process of the aluminate  $12\text{CaO}\cdot 7\text{Al}_2\text{O}_3$ -assisted Portland cement-based solidification/stabilization of sewage sludge, *Construction and Building Materials* 30 (2012), pp. 675–681.

**Table 1.** Detailed composition of the mortar samples assayed.

<i>Raw material</i>	<i>Control*</i>	<i>WS-1</i>	<i>WS-2</i>	<i>WS-3</i>	<i>WS-4</i>	<i>WS-5</i>	<i>BS-1</i>	<i>BS-2</i>	<i>BS-3</i>	<i>BS-4</i>	<i>BS-5</i>
<i>Sludge (g)</i>	.*	39	78	117	156	195	39	78	117	156	195
<i>Ratio S/CAC (wt %)</i>	20	10	20	30	40	50	10	20	30	40	50
<i>CAC (g)</i>	390	390	390	390	390	390	390	390	390	390	390
<i>Sand (g)</i>	610	610	610	610	610	610	610	610	610	610	610
<i>Water (wt %)</i>	10.50	15.00	18.20	21.50	22.50	23.50	14.43	18.00	19.50	19.50	20.50

\* Control sample was prepared by mixing 78 g of pure sodium hexametaphosphate (SHMP) as a source of pure phosphate.

**Table 2.** Chemical composition of the sludges.

<i>Component</i>	<i>WS</i>	<i>BS</i>
<i>Organic matter (wt %)</i>	21.6 ± 0.1	29.7 ± 0.1
<i>Major elements (wt %)</i>		
<i>P (as PO<sub>4</sub><sup>3-</sup>)</i>	49.0 ± 2.5	20.0 ± 0.4
<i>Fe</i>	21.6 ± 1.0	12.7 ± 0.8
<i>Ca</i>	0.31 ± 0.02	14.25 ± 0.08
<i>CO<sub>3</sub><sup>2-</sup></i>	< LOD	10.17 ± 0.01
<i>Zn</i>	4.5 ± 0.2	2.0 ± 0.2
<i>SO<sub>4</sub><sup>2-</sup></i>	1.20 ± 0.04	0.10 ± 0.02
<i>Mn</i>	0.86 ± 0.05	0.75 ± 0.01
<i>Ni</i>	0.51 ± 0.03	0.64 ± 0.01
<i>Na</i>	0.46 ± 0.03	0.13 ± 0.01
<i>Mg</i>	0.012 ± 0.001	0.334 ± 0.014
<i>Al</i>	0.19 ± 0.01	0.26 ± 0.01
<i>K</i>	0.29 ± 0.02	0.26 ± 0.01
<i>Ti</i>	0.014 ± 0.001	0.218 ± 0.003
<i>Cu</i>	0.128 ± 0.008	0.039 ± 0.001
<i>Minor elements (mg Kg<sup>-1</sup>)</i>		
<i>Cr</i>	382 ± 21	143 ± 6
<i>Pb</i>	48 ± 1	46 ± 2
<i>Cd</i>	2.4 ± 0.2	4.4 ± 0.4

**Table 3.** pH and conductivity values measured in a 1:5 weight ratio aqueous sludge suspensions.

<i>Parameter</i>	<i>WS</i>	<i>BS</i>
<i>pH</i>	5.47 ± 0.01	5.46 ± 0.01
<i>Conductivity (μS cm<sup>-1</sup>)</i>	2740 ± 1	1500 ± 1

**Table 4.** Results of the consistency of the fresh mortars (slump values obtained in the flow table test) and setting time.

<i>Raw material</i>	<i>Control</i>	<i>WS-1</i>	<i>WS-2</i>	<i>WS-3</i>	<i>WS-4</i>	<i>WS-5</i>	<i>BS-1</i>	<i>BS-2</i>	<i>BS-3</i>	<i>BS-4</i>	<i>BS-5</i>
<i>Slump (mm)</i>	138	134	141	130	143	126	130	145	140	144	128
<i>Setting time (min)</i>	6	9	15	23	55	62	7	31	50	83	100

**Table 5.** Total porosity values of the tested mortars.

<i>Parameter</i>	<i>Control</i>	<i>WS-1</i>	<i>WS-2</i>	<i>WS-3</i>	<i>WS-4</i>	<i>WS-5</i>	<i>BS-1</i>	<i>BS-2</i>	<i>BS-3</i>	<i>BS-4</i>	<i>BS-5</i>
<i>Porosity (%)</i>	8.7	13.9	17.7	26.3	30.2	27.4	19.2	18.1	24.2	18.6	23.5

**Table 6.** Potential risk evaluation of leaching of potentially toxic constituents of sludges (extraction test method EN 12457-4 under aqueous and acidic solution) and leaching limit values for landfilling of hazardous waste (2003/33/EC).

<i>Analyte</i>	<i>WS</i>		<i>BS</i>		<i>Leaching limit value</i>
	<i>H<sub>2</sub>O</i>	<i>HCl 0.1M</i>	<i>H<sub>2</sub>O</i>	<i>HCl 0.1M</i>	
<i>Zn (mg L<sup>-1</sup>)</i>	243.7±0.7	1341±7	0.40±0.06	0.78±0.02	60
<i>Cu (mg L<sup>-1</sup>)</i>	0.49±0.02	0.61±0.07	0.29±0.01	0.29±0.01	60
<i>Ni (mg L<sup>-1</sup>)</i>	82±4	217±9	2.14±0.01	18±1	12
<i>Cr (mg L<sup>-1</sup>)</i>	0.03±0.01	0.32±0.03	0.004±0.001	0.03±0.01	15
<i>Mn (mg L<sup>-1</sup>)</i>	79±6	333±10	0.33±0.03	13.9±0.7	-
<i>TOC (mg L<sup>-1</sup>)</i>	47.4±0.1	-	427.7±0.1	-	320

**Table 7.** Efficiency of the solidification/stabilization process in terms of retention percentages (% R) and total cumulative leaching (expressed in mg of analysed elements per unit of specimen surface area, m<sup>2</sup>) after performing the semi-dynamic tank test in monolithic specimens.

<i>WS mortars</i>										
	<i>WS-1</i>		<i>WS-2</i>		<i>WS-3</i>		<i>WS-4</i>		<i>WS-5</i>	
	% R	leaching	% R	leaching	% R	leaching	% R	leaching	% R	leaching
<b><i>PO<sub>4</sub><sup>3-</sup></i></b>	99.82	481.6	99.95	238.4	99.97	246.3	99.95	435.7	99.97	408.2
<b><i>Zn</i></b>	99.97	4.66	99.99	4.16	99.99	2.58	99.99	2.22	99.99	2.42
<b><i>Cr</i></b>	100.0	<LOD	98.39	6.83	92.50	42.85	95.81	35.47	97.68	24.59
<b><i>Ni</i></b>	99.42	16.44	99.69	17.55	99.60	33.84	99.83	18.87	99.86	19.87
<b><i>Cu</i></b>	99.59	2.00	99.68	4.61	99.83	3.56	99.85	4.40	99.92	2.85
<b><i>Mn</i></b>	100.0	<LOD	100.0	<LOD	100.0	<LOD	100.0	<LOD	100.0	<LOD

<i>BS mortars</i>										
	<i>BS-1</i>		<i>BS-2</i>		<i>BS-3</i>		<i>BS-4</i>		<i>BS-5</i>	
	% R	leaching	% R	leaching	% R	leaching	% R	leaching	% R	leaching
<b><i>PO<sub>4</sub><sup>3-</sup></i></b>	99.95	48.88	99.76	529.92	99.94	332.62	99.92	461.87	99.94	451.15
<b><i>Zn</i></b>	99.97	4.65	99.98	4.37	99.99	2.24	99.99	2.24	99.99	1.37
<b><i>Cr</i></b>	96.19	3.02	96.16	8.09	98.64	3.24	100.0	< LOD	99.86	0.57
<b><i>Ni</i></b>	99.85	5.22	99.29	30.28	99.94	5.61	99.98	2.35	99.97	4.61
<b><i>Cu</i></b>	98.13	4.06	99.58	4.82	94.65	35.00	95.90	35.78	97.03	32.39
<b><i>Mn</i></b>	100.0	< LOD	100.0	< LOD	100.0	< LOD	100.0	< LOD	100.0	< LOD

**Table 8.** Total organic carbon values (mg L<sup>-1</sup>) found in leachates after performing the semi-dynamic tank test in monolithic specimens.

	<i>TOC</i>		<i>TOC</i>
<b><i>WS-1</i></b>	4.8 ± 0.1	<b><i>BS-1</i></b>	3.3 ± 0.1
<b><i>WS-2</i></b>	2.7 ± 0.1	<b><i>BS-2</i></b>	3.4 ± 0.1
<b><i>WS-3</i></b>	2.4 ± 0.1	<b><i>BS-3</i></b>	3.8 ± 0.1
<b><i>WS-4</i></b>	2.2 ± 0.1	<b><i>BS-4</i></b>	4.1 ± 0.1
<b><i>WS-5</i></b>	2.0 ± 0.1	<b><i>BS-5</i></b>	5.7 ± 0.1

**Table 9.** Slopes ( $\pm$ s.d.) of the log–log plots of derived cumulative leaching at the representative increment 2-7 of the diffusion test (the dissolution process governs the leaching mechanism when the slope reach a value higher than 0.65).

<i>Sludge</i>	<i>Ca</i>	<i>P</i>	<i>Zn</i>
<i>WS-1</i>	0.880 $\pm$ 0.104	0.660 $\pm$ 0.091	0.828 $\pm$ 0.188
<i>WS-2</i>	0.922 $\pm$ 0.143	0.869 $\pm$ 0.136	0.807 $\pm$ 0.098
<i>WS-3</i>	1.135 $\pm$ 0.148	0.591 $\pm$ 0.095	0.690 $\pm$ 0.063
<i>WS-4</i>	1.093 $\pm$ 0.202	0.715 $\pm$ 0.083	0.749 $\pm$ 0.073
<i>WS-5</i>	1.000 $\pm$ 0.127	0.321 $\pm$ 0.038	0.633 $\pm$ 0.078
<i>BS-1</i>	0.730 $\pm$ 0.077	0.837 $\pm$ 0.089	0.742 $\pm$ 0.105
<i>BS-2</i>	0.883 $\pm$ 0.129	0.745 $\pm$ 0.105	0.682 $\pm$ 0.094
<i>BS-3</i>	0.831 $\pm$ 0.129	0.554 $\pm$ 0.090	0.590 $\pm$ 0.089
<i>BS-4</i>	0.875 $\pm$ 0.096	0.807 $\pm$ 0.055	0.921 $\pm$ 0.155
<i>BS-5</i>	0.730 $\pm$ 0.077	0.660 $\pm$ 0.038	1.120 $\pm$ 0.217

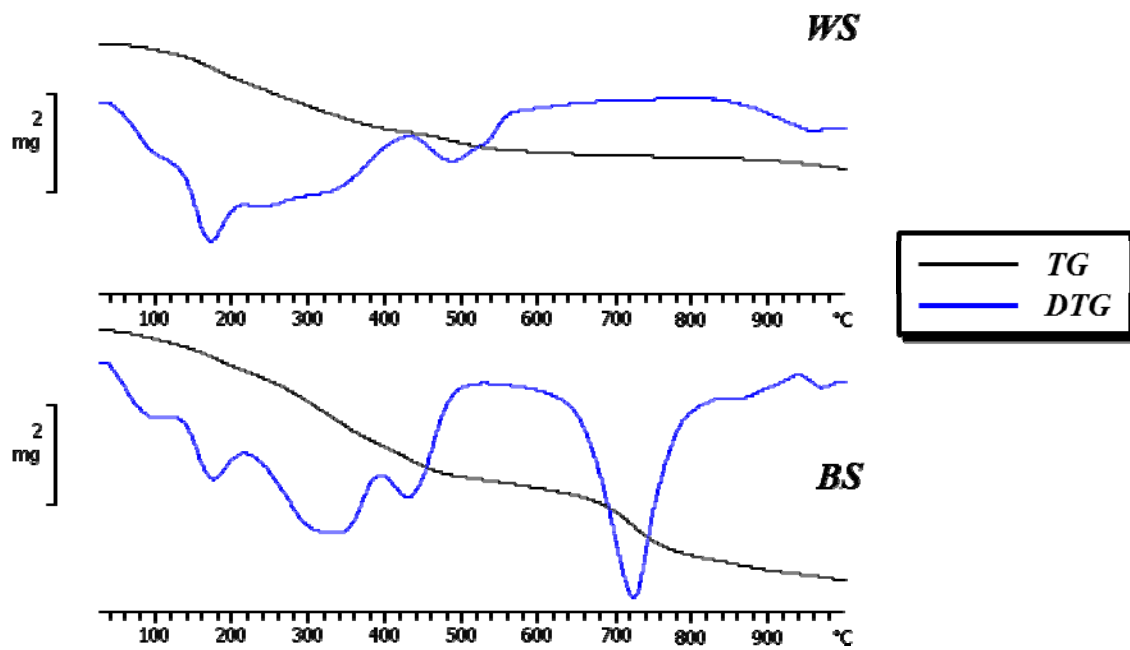


**Figure 1.** TG and DTG curves for WS and BS samples.

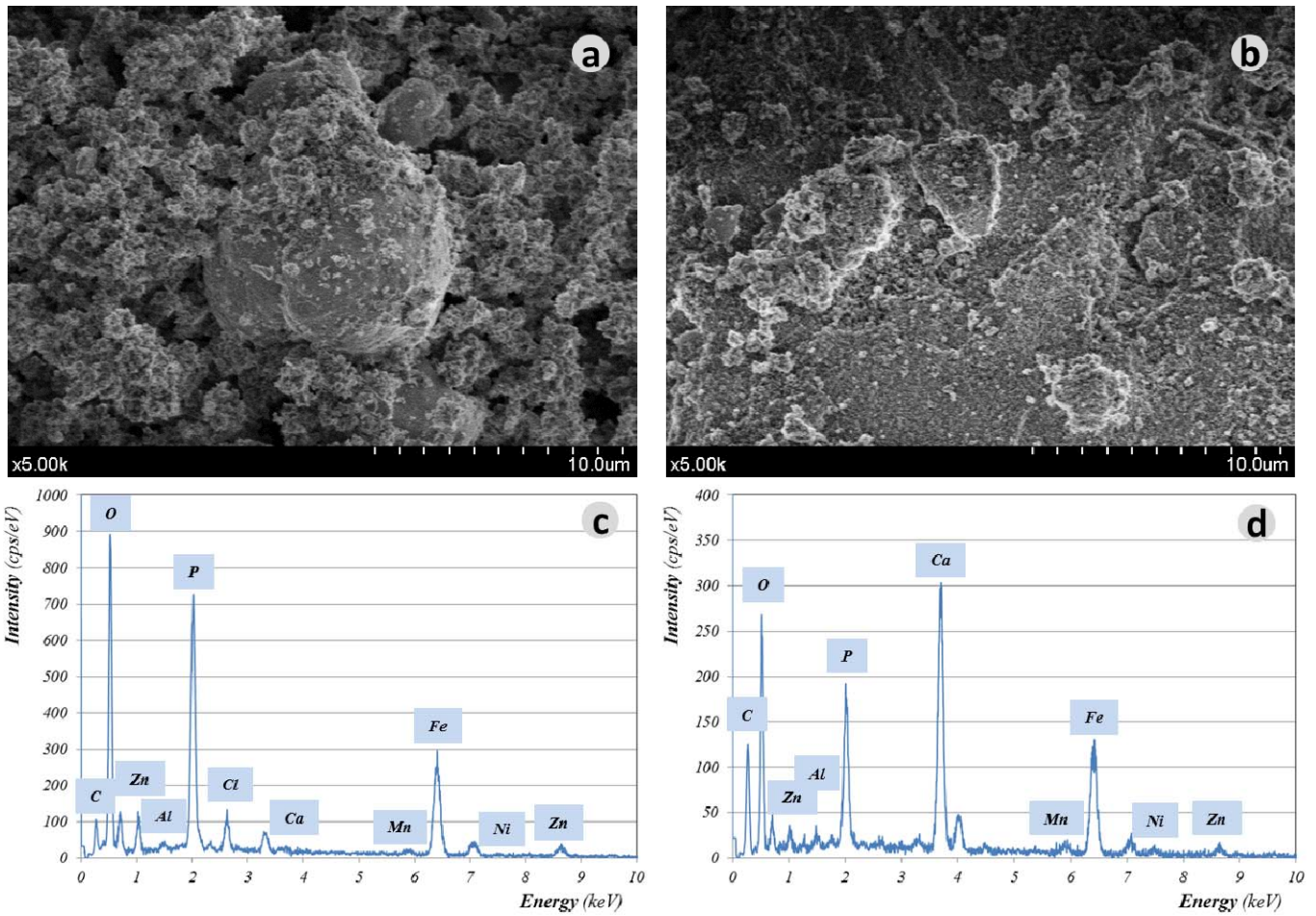


**Figure 2.** SEM micrographs for the untreated sludges: a) WS and b) BS. EDAX elemental chemical composition of c) WS and d) BS.

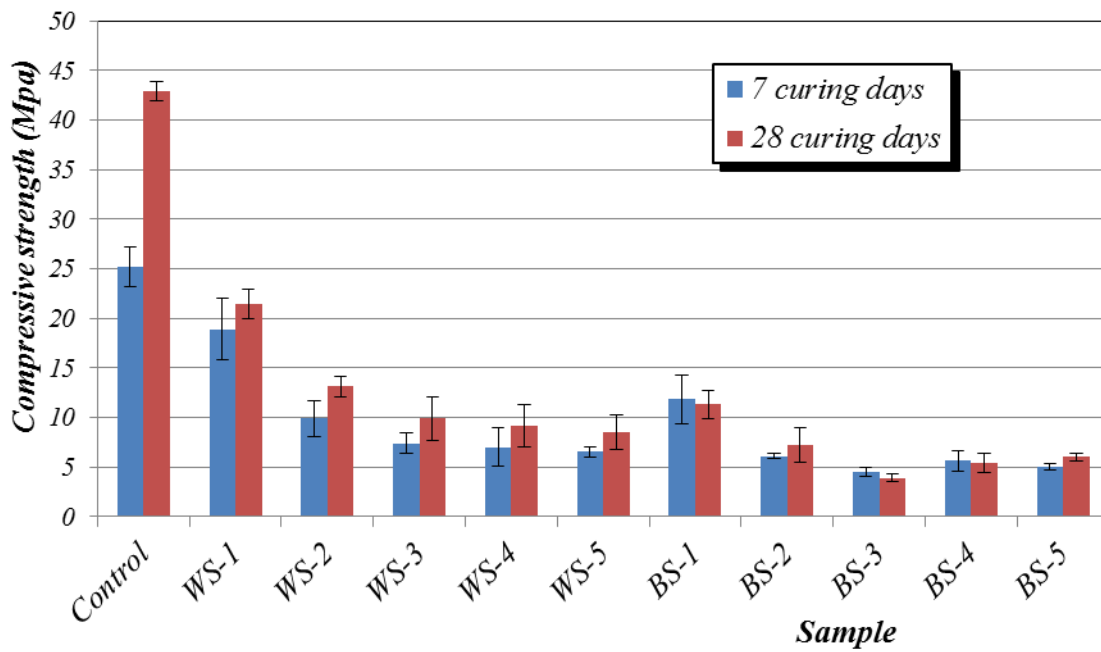


**Figure 3.** Compressive strengths (MPa) for PS-CAC mortars at 7 and 28 curing days.

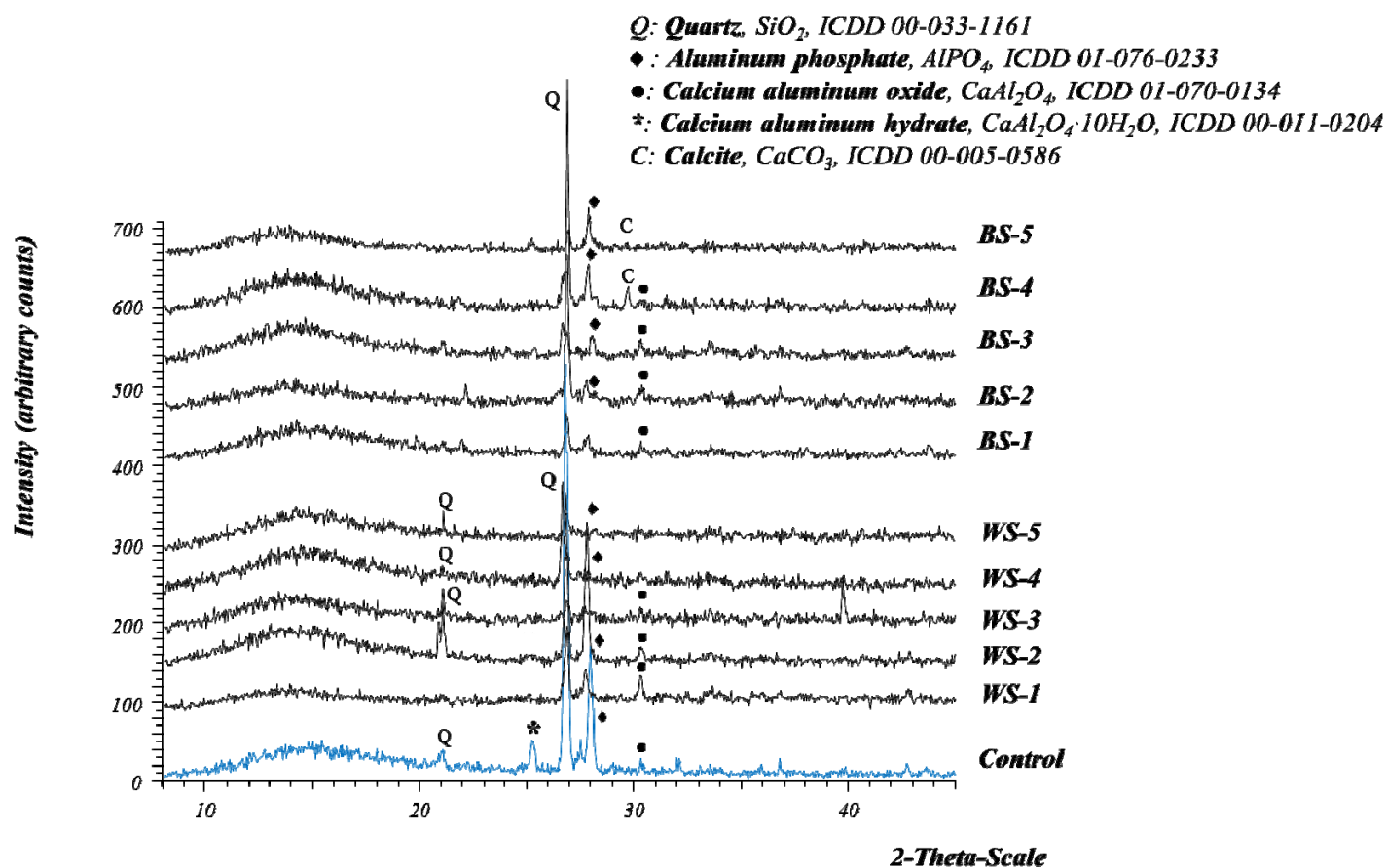


**Figure 4.** XRD patterns of the samples after 28 curing days.



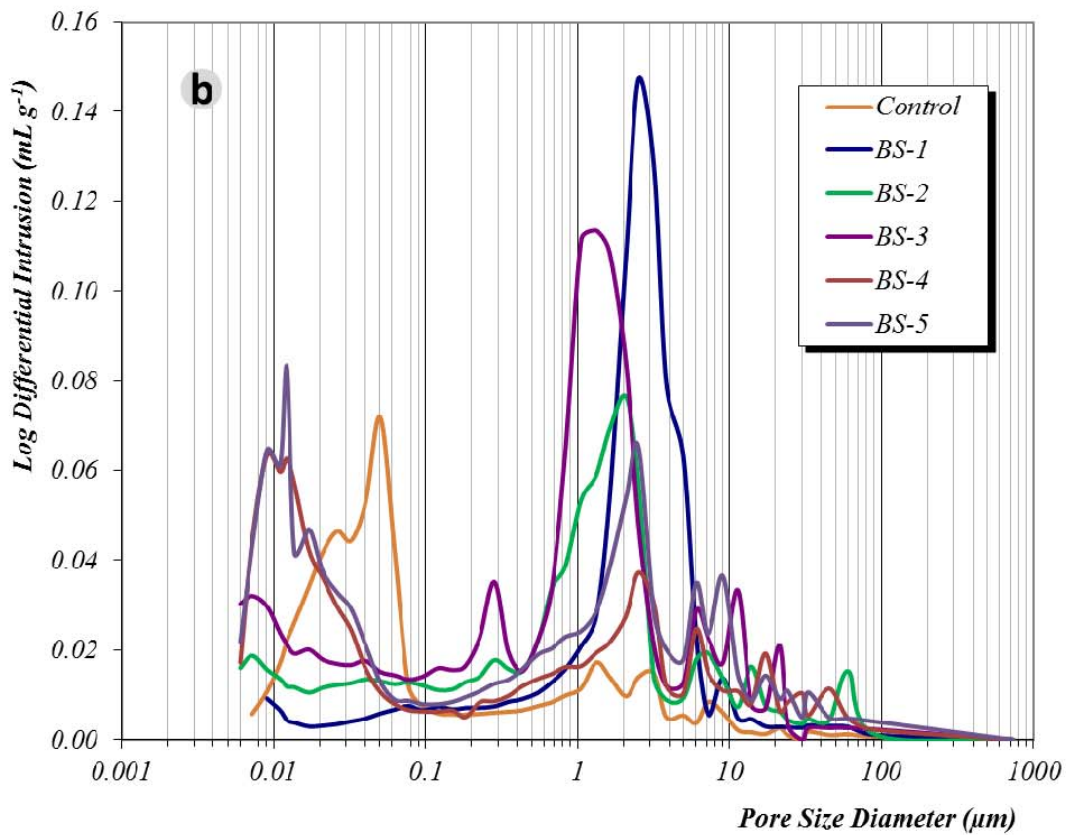
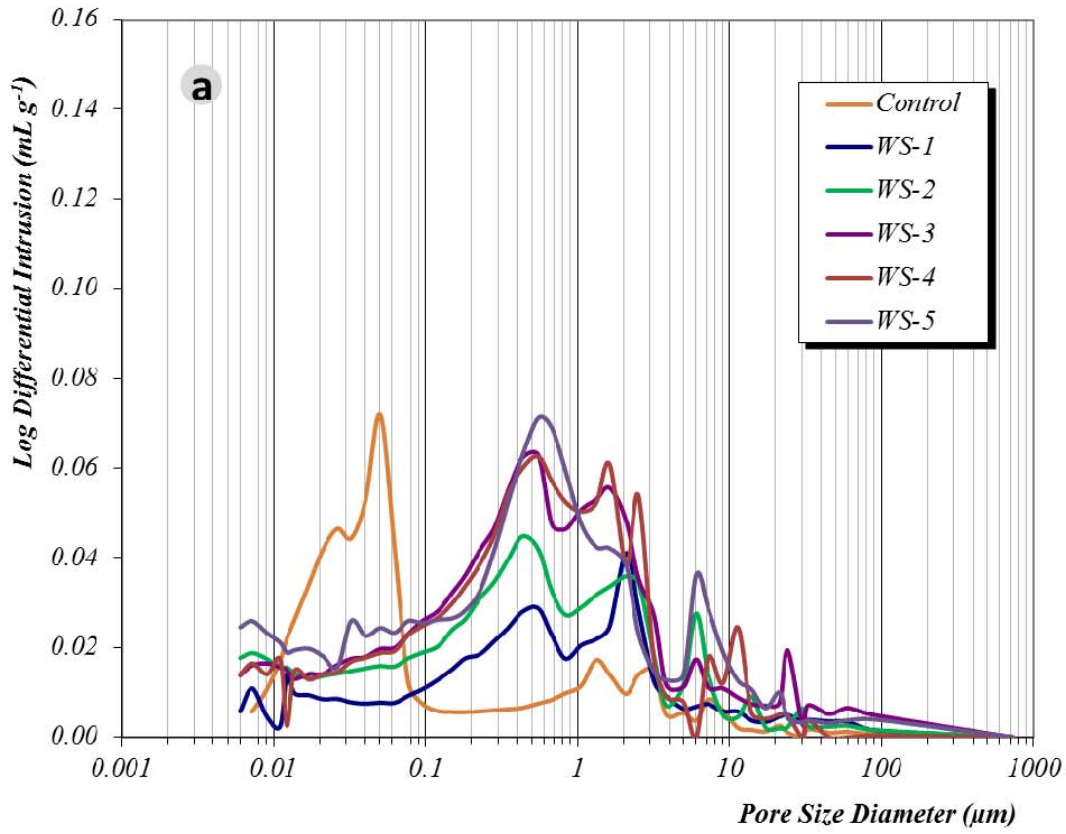


**Figure 5.** Pore size distributions of a) WS and b) BS mortars after 28 curing days.

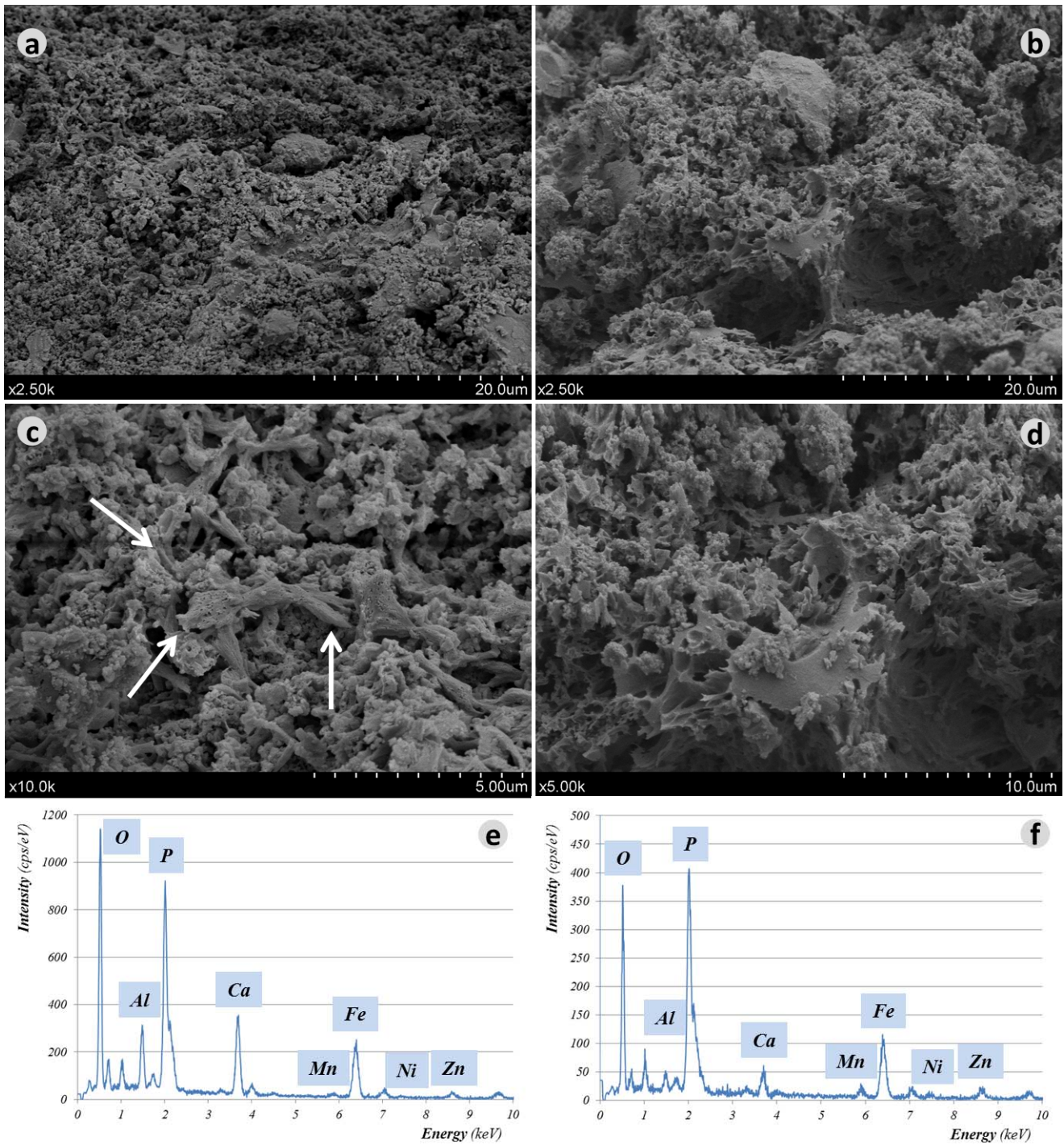


**Figure 6.** SEM micrographs: a) WS-1 sample; b) WS-5 sample; c) detailed micrograph of WS-1, with a fibrous network of ACP (arrows); d) different area of WS-1 showing ACP as a honeycomb-shaped microstructure; e) and f) EDAX profiles of the (c) and (d) micrographs, respectively, with simultaneous presence of P, Ca and Zn.

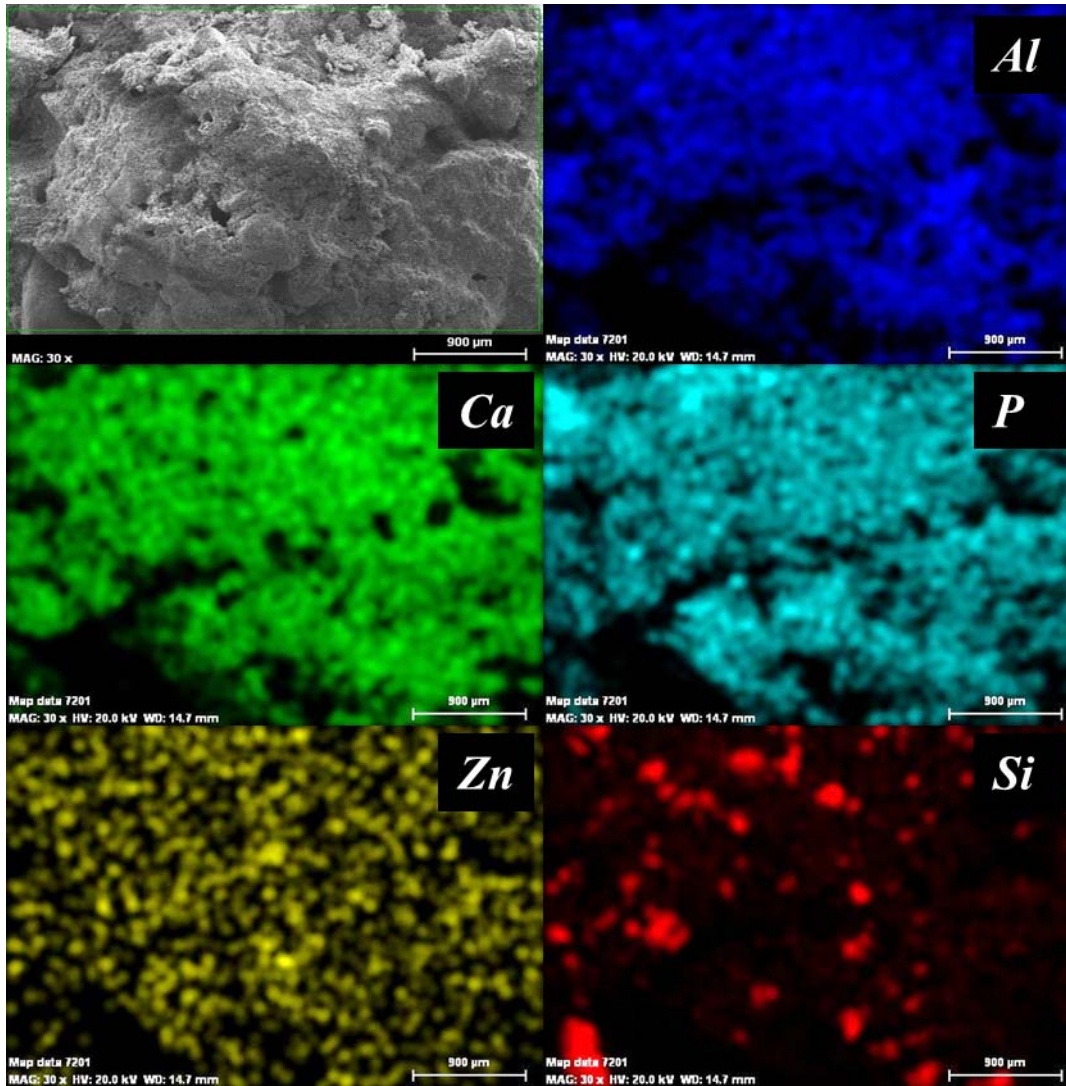


**Figure 7.** Elemental mapping of WS-5 sample.



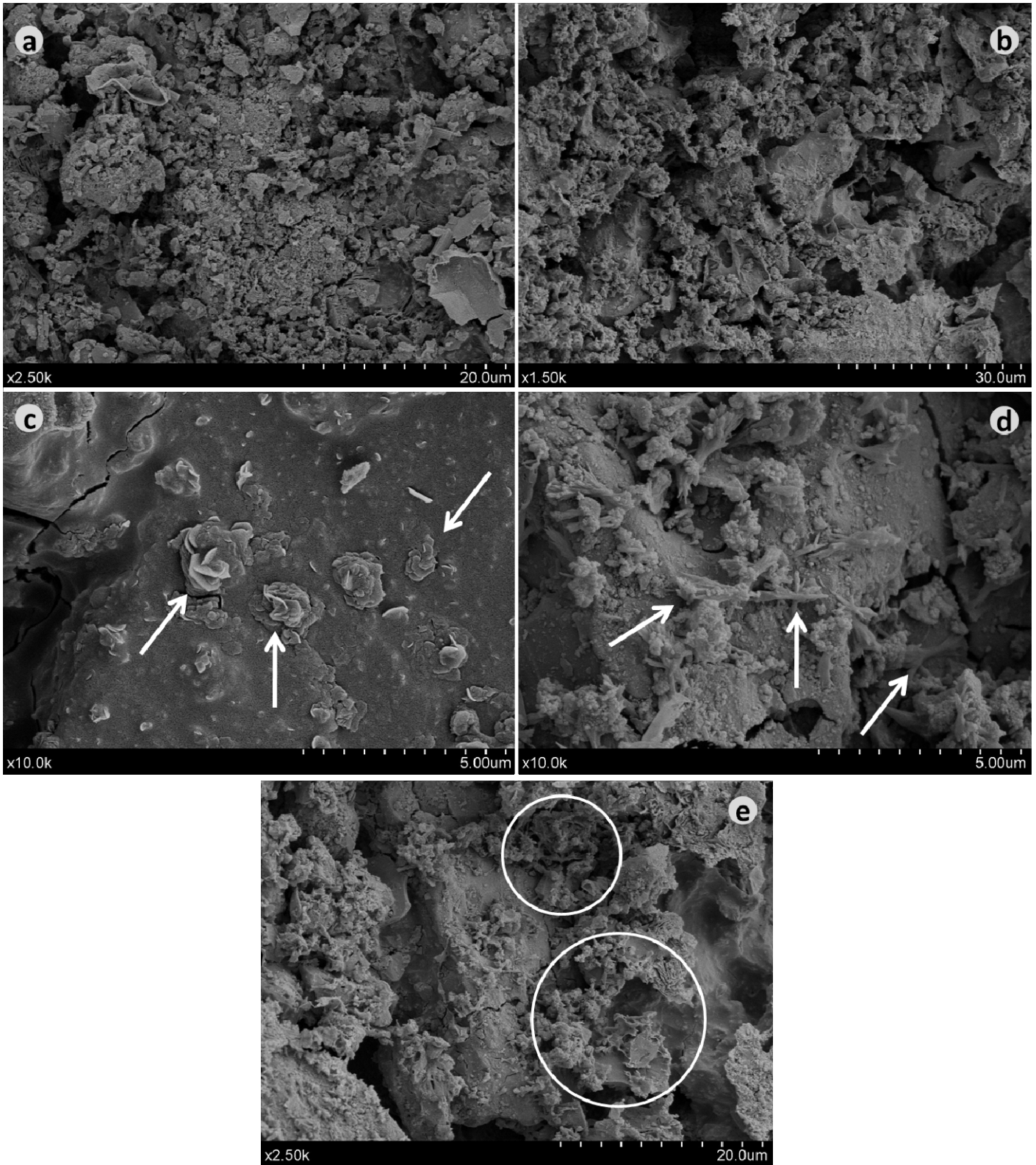


**Figure 8.** SEM micrographs: a) BS-1 sample; b) BS-5 sample with larger porosity; c) detailed image of BS-1 sample showing some hexagonal platelets of  $CAH_{10}$ , indicated by arrows; d) BS-5 sample with fibrous ACP (pointed by arrows); and e) area of BS-5 where ACP is shown as honeycomb-shaped microstructure.

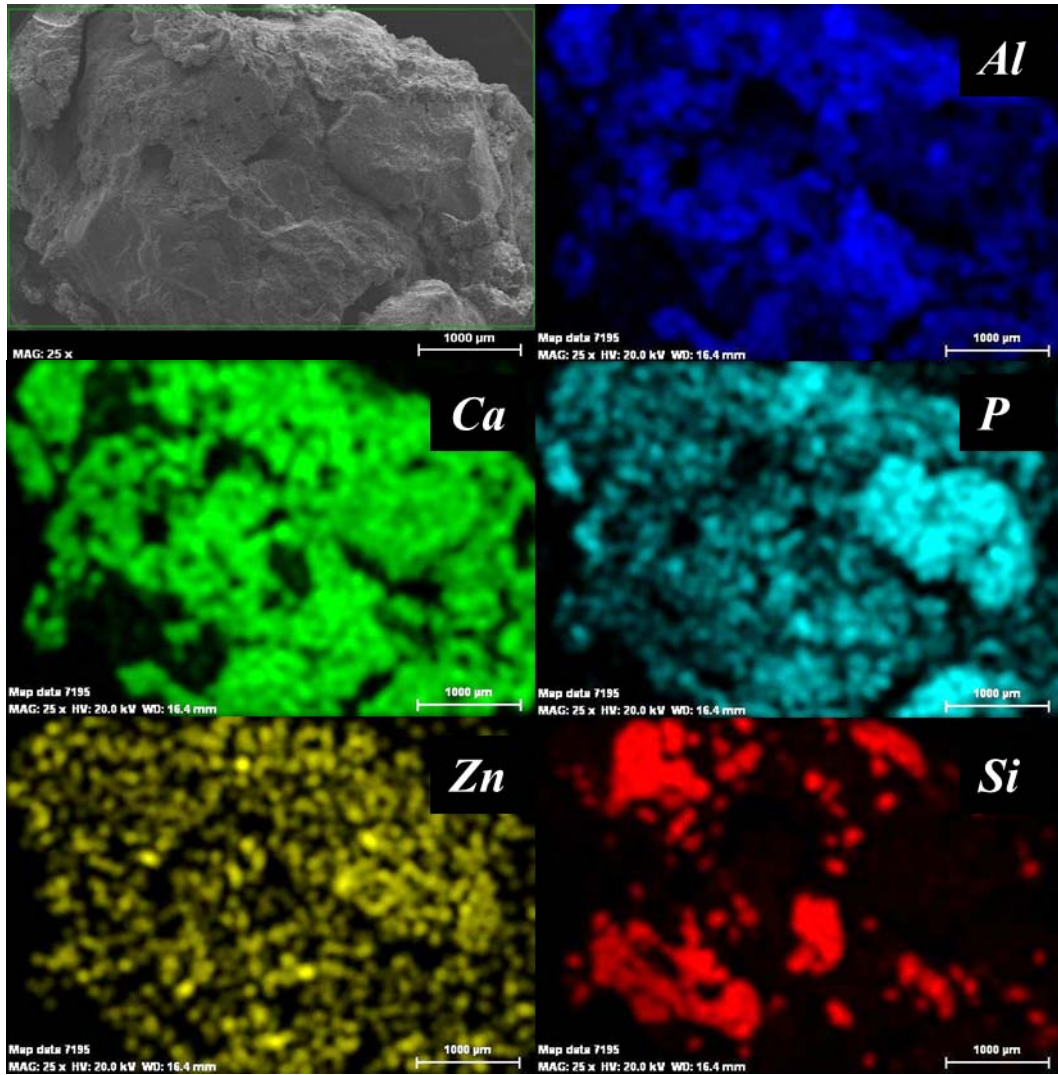
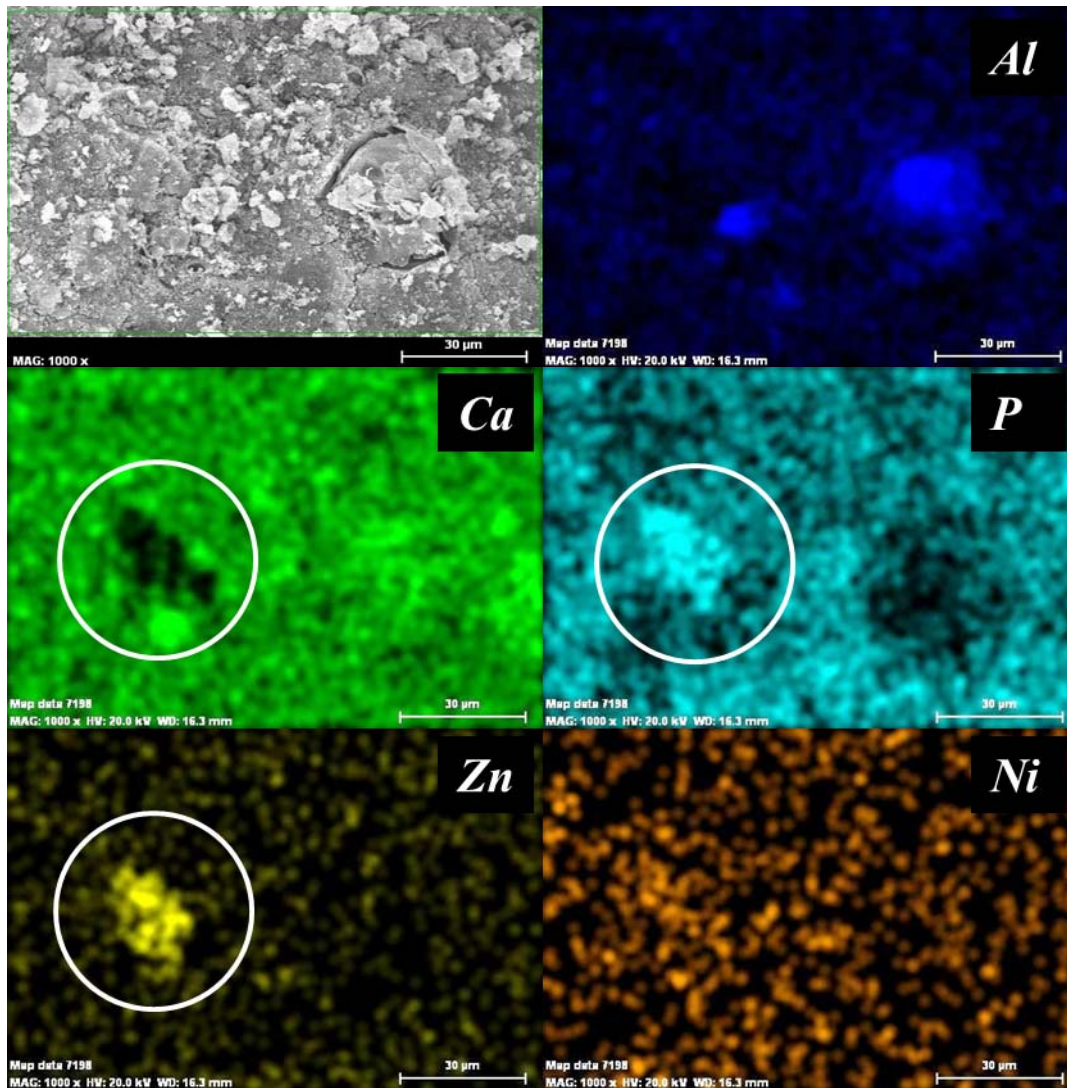


Figure 9. Elemental mapping of BS-5 sample.



**Figure 10.** Elemental mapping of a different area of BS-5 sample. Spots of unreacted Zn phosphates appeared as the brightest areas and are encircled in the mapping images of P and Zn. The absence of interaction was simultaneously proved by the darkest area in the Ca image, also indicated with a circle.



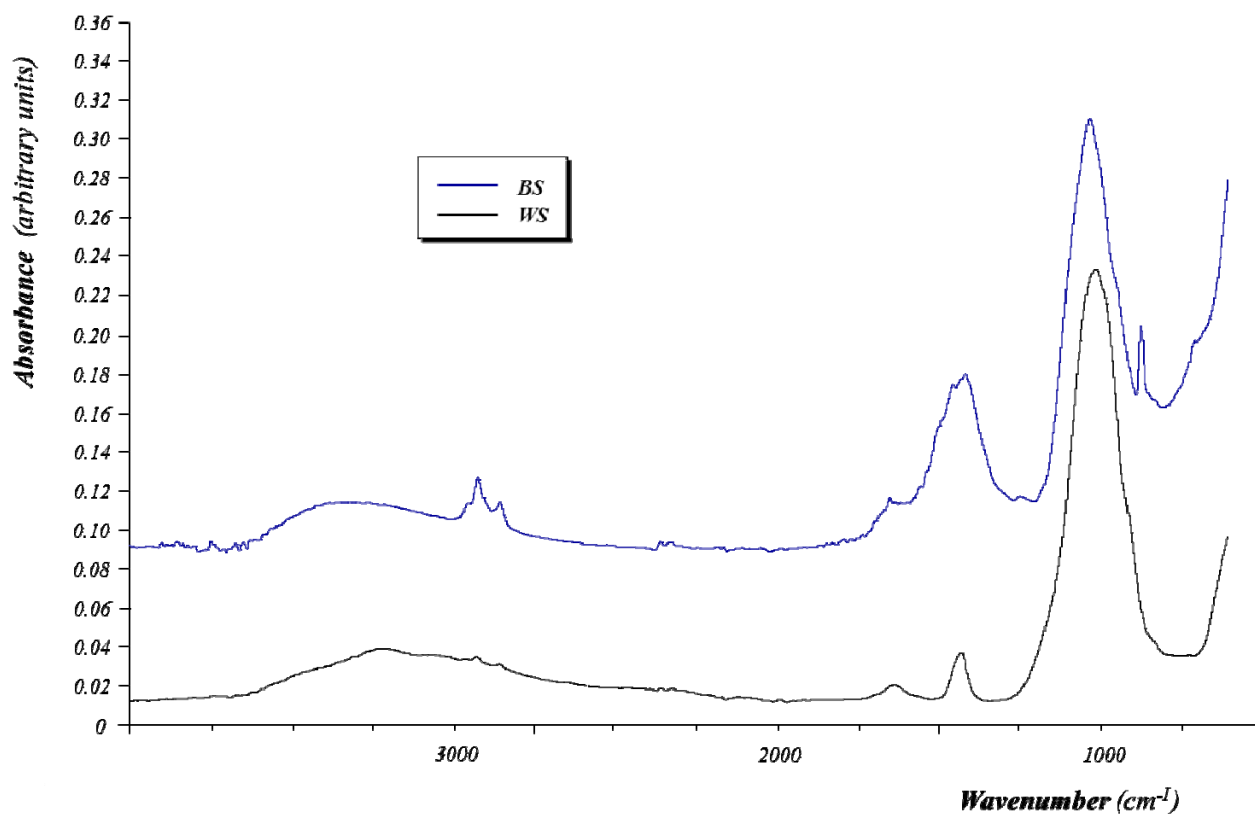


Figure S1. FTIR-ATR spectra of both sludges analysed.

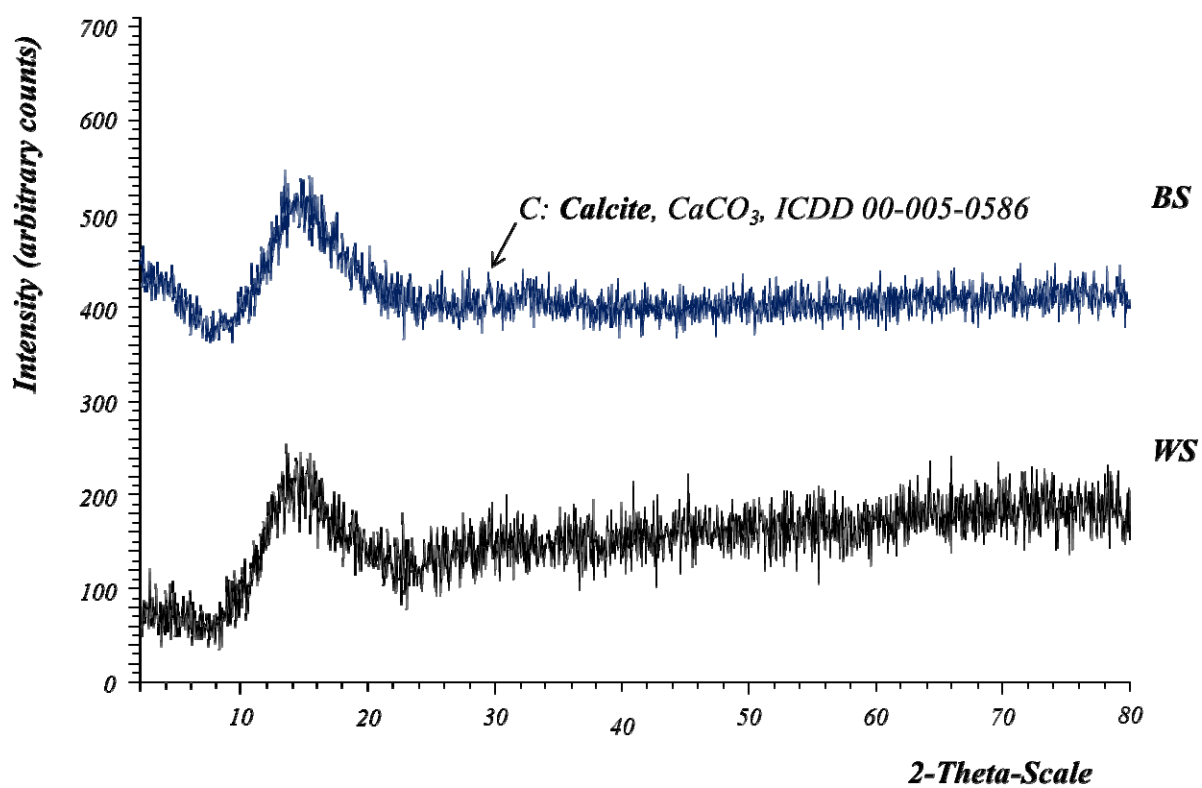


Figure S2. XRD profile for both sludges analysed.